Experimental Studies on the Aggregation Properties of Ice and Dust in Planet-Forming Regions

Daniel Heißelmann
Institut für Geophysik und extraterrestrische Physik, Technische Universität zu Braunschweig, Mendelssohnstraße 3, D-38106 Braunschweig, Germany
d.heisselmann@tu-bs.de,

Helen J. Fraser
Department of Physics, University of Strathclyde, John Anderson Building, 107 Rottenrow, Glasgow G4 0NG, United Kingdom
h.fraser@phys.strath.ac.uk,

and

Jürgen Blum
Institut für Geophysik und extraterrestrische Physik, Technische Universität zu Braunschweig, Mendelssohnstraße 3, D-38106 Braunschweig, Germany
j.blum@tu-bs.de

Abstract

To reveal the formation of planetesimals it is of great importance to understand the collision behavior of the dusty and icy aggregates they have formed from. We present an experimental setup to investigate the aggregation properties in low-velocity collisions of dust aggregates, solid ices and icy aggregates under microgravity conditions. Results from ESA's 45$^{\rm th}$ Parabolic Flight Campaign show that most collisions in the velocity range $0.1\,{\rm m\,s^{-1}} \lesssim v_c \lesssim 0.5\,{\rm m\,s^{-1}}$ are dominated by a rebound behavior of the projectile dust aggregates and only $\sim 5\%$ of the translational kinetic energy is conserved after the encounters.

1 Introduction

Current theories say that stars form from gravitational collapse of dense, turbulent, and rotating molecular clouds. This contraction occurs when the gas pressure can no longer support the cloud core against gravity. After the formation of a central protostar the gas environment cools down and allows for the condensation of (sub-) micrometer-sized mineral grains. Due to the conservation of angular momentum dust is accreted along the rotational axis of the system by the new-born star whereas perpendicular to this axis a flattened, differentially rotating accretion disk develops. In the protoplanetary disk, which typically has a dust-to-gas ratio of ~ 0.01, matter can only be transported towards the center of gravity as a result of friction forces, which are thought to be caused by gas turbulence or magneto-rotational turbulence. According to the model of Weidenschilling and Cuzzi (1993), inelastic collisions of dust grains combined with adhesive surface forces (van-der-Waals forces or hydrogen bonding) between colliding particles cause them to coagulate by a hit-and-stick method. The relative velocities of the colliding grains or agglomerates are the result of Brownian motion (Brown, 1828; Einstein, 1905), relative drift motion of two particles or gas turbulence (Weidenschilling and Cuzzi, 1993). In this scenario Brownian motion is most important for small dust aggregates of sizes between $\sim 1\,\mu$m and $\sim 100\,\mu$m while collisions of larger aggregates are dominated by gas turbulence and drift towards the center of gravity (Weidenschilling and Cuzzi, 1993).

The so-formed agglomerates become more compact due to restructuring in more energetic collisions which occur due to the increasing relative velocities with increasing agglomerates masses. When the particles have become more compact they decouple from the protoplanetary disk's gas and sedimentation to the mid-plane causes the onset of the runaway-growth phase (Weidenschilling and Cuzzi, 1993; Weidenschilling, 1997) in which larger aggregates increase their size dramatically by sweeping-up smaller agglomerates while sedimentating.

As soon as planetesimals of $s \gtrsim 1\,\mathrm{km}$ have formed the collisions between those bodies are dominated by gravity. Gravitational perturbations accelerate the smaller planetesimals leading to high-velocity collisions between kilometer-sized bodies. These encounters result in collisional fragmentation from which the environment of the larger planetesimals is fed with smaller fragments. Capturing of fragments by larger runaway bodies then allows the rapid growth to Mercury size on a $\sim 10^5$-years time scale (Wetherill and Stewart, 1989, 1993).

However, the growth of kilometer-sized planetesimals from millimeter to centimeter-sized aggregates is still an unanswered question. Sect. 2 of this manuscript gives an overview of the numerous simulations and experimental studies on the formation of planetesimals which have been carried out within the past decades. In Sect. 3 the scientific objectives of the experiments performed here are described and Sect. 4 gives a detailed description of the setup used for studying low-velocity collisions of dust aggregates. The results obtained during ESA's 45$^{\mathrm{th}}$ Parabolic Flight Campaign and their interpretation can be found in Sect. 5. In Sect. 6 several intended improvements to the experiment setup and procedures are explained.

2 Previous Work

In the past decades numerous laboratory experiments and numerical simulations were performed to reveal the processes involved in the formation of the terrestrial planets, the asteroids and the cores of the giant planets.

Weidenschilling and Cuzzi (1993) present a model which describes the formation of planetesimals from fractal dust aggregates which have formed in the collisions of single, (sub-) micrometer-sized dust grains (Meakin and Donn, 1988; Blum, 2004; Krause and Blum, 2004).

In numerical simulations Dominik and Tielens (1997) studied the interaction forces of two colliding aggregates of fractal structure, which consist of equal-sized, spherical monomers. They considered the adhesion forces, the rolling and the sliding between all pairs of grains which are in contact inside the two colliding aggregates. The outcome of their calculations is that the key parameters in collisions of fractal aggregates are the number of monomer-monomer contacts within both aggregates, the energy required to break-up a grain-grain contact and the rolling-friction energy which is necessary to roll two neighboring grains by one quarter of their circumference. With increasing collision velocity and thus with increasing impact energy, Dominik and Tielens distinguish between five regimes: (1) a hit-and-stick behavior in which sticking occurs without restructuring of the aggregates, (2) the beginning of restructuring resulting in compaction of the aggregates until (3) a state of maximum compaction is achieved. At even higher impact velocities (4) the break-up of grain-grain bonds occurs and finally results in (5) the catastrophic disruption of the aggregates. Blum and Wurm (2000) experimentally showed that this model is correct and measured at which collision velocities the various stages occur.

Wurm and Blum (1998) present results from laboratory experiments probing the collisions of fluffy, fractal aggregates ($D_f \approx 1.91$, where $m \propto r^{D_f}$ and m, r, and D_f are the mass, the radius of gyration and the fractal dimension, respectively) consisting of monodisperse spherical SiO_2 grains ($s_0 = 1.9\,\mu$m). They found that in the collision velocity range of $0.001\,\mathrm{m\,s^{-1}} \lesssim v_c \lesssim 0.01\,\mathrm{m\,s^{-1}}$ the sticking probability is unity and no restructuring or compaction of the constituent aggregates occurs.

Blum and Schräpler (2004) and Blum et al. (2006) built large, compact ($D_f \approx 3$) dust agglomerates from $1.5\,\mu$m-sized SiO_2 grains, which can be considered as planetesimal analogue bodies. These agglomerates – so-called 'dust cakes' – are produced by the method of Random Ballistic Deposition (RBD) in which first dust powder is de-agglomerated to its micrometer-sized constituent grains, secondly the grains are coupled to a gas flow and finally they are unidirectionally deposited on a filter. By using this technology planetesimal-analog aggregates of 2.5 cm diameter and up to 2 cm in height can be built.

Blum and Schräpler (2004) and Blum et al. (2006) showed that these aggregates have a highly porous structure. In unidirectional compression experiments the volume filling factor $\phi = \frac{\varrho}{\varrho_0}$ (where ϱ is the aggregate's density and ϱ_0 is the bulk density of the constituent monomer grains) as a function of the applied pressure increased asymptotically from $\phi = 0.07...0.15$ to $\phi \lesssim 0.20...0.33$.

Langkowski et al. (2007) recently carried out microgravity experiments to investigate the collision behavior of $s \sim 0.1 - 1$ mm-sized high-porosity dust-aggregates (projectile) and 2.5 cm-sized target of the same material in the velocity regime of $0.5 - 3\,\mathrm{m\,s^{-1}}$. They found that near-normal collisions were dominated by sticking while near-tangential impacts showed rebounding behavior of the projectiles. For collisions which did not result in sticking of the projectile Langkowski et al. observed a mass transfer from the target to the projectile which approximately doubled the projectile's mass.

Laboratory collision experiments with pairs of 1 mm-sized aggregates at velocities of 0.15 to $3.9\,\mathrm{m\,s^{-1}}$ were carried out by Blum and Münch (1993). They used aggregates consisting of $s_0 = 0.2...1\,\mu$m-sized $ZrSiO_4$ monomers which have a volume filling factor of $\phi = 0.26$ and collided them at arbitrary impact angles. It was found that low-velocity encounters resulted in rebounding of the projectile aggregates, whereas at $v_c \gtrsim 1\,\mathrm{m\,s^{-1}}$ a transition to fragmentation was observed. For the bouncing aggregates the coefficient of restitution ϵ – the ratio of relative velocities after and before the collision – and the normalized translational energy ϵ^2 were determined. The results showed that for central collisions the conserved translational energy was at $\sim 10\%$ of the value before the collision. For perfectly grazing encounters a theoretical value for the conserved kinetic energy of $\epsilon_t^2 = 0.51$ was calculated. Furthermore, Blum and Münch observed that collisions at velocities exceeding $\sim 3\,\mathrm{m\,s^{-1}}$ were followed by complete disruption of the initial impactors with the number of fragments following a power-law mass distribution.

In addition to silicates, water ices (and other condensates of volatiles, like e.g. CO, CO_2, NH_3, CH_3OH and CH_4), which are ubiquitous in the outer reaches of the solar nebula, are of great importance for the formation of Pluto, the comets, the Kuiper belt objects (KBOs) and the icy moons of the giant planets. However, only very limited knowledge exists on the aggregation properties of ices in the solar nebula and detailed studies of the collision behavior and fragmentation thresholds of icy agglomerates (Ehrenfreund et al., 2003; Fraser et al., 2005).

To probe the collision properties of icy bodies as they are found in Saturn's rings, Bridges et al. (1984) and Hatzes et al. (1988) performed quasi-2D collision experiments between solid ice spheres of several centimeters in diameter and at very low relative velocities of $1.5 \cdot 10^{-4} - 2 \cdot 10^{-2}\,\mathrm{m\,s^{-1}}$. They found that the coefficient of restitution ϵ follows an exponential law of the type $\epsilon\,(v_c) = C \cdot \exp\,(-\gamma v_c)$. It was also discovered that the values of ϵ strongly depend on the properties of the contact surfaces and can be lowered by up to 30% as a result of roughened or frosted surfaces. Hatzes et al. conclude that, except for particles with a very smooth surface, a size dependence exists in the coefficient of restitution, ϵ.

3 Scientific Objectives

The goal of our experiments is to analyze if and how millimeter-sized dust aggregates, solid ices and icy aggregates stick together (i.e. form aggregates) in a microgravity environment that best simulates the protoplanetary disks where these particles combine to form planetesimals and cometary nuclei. Therefore, we carry out collisions of pairs of $2-5$ mm-sized projectiles probing mutual collisions of similar sized aggregates in protoplanetary disks. To simulate collisions of different sized bodies the impacts of aggregates on a larger solid target can also be observed. In both types of experiments the collisions occur at low velocities of $0.1\,\mathrm{m\,s^{-1}} \lesssim v_c \lesssim 0.5\,\mathrm{m\,s^{-1}}$ which are the typical relative velocities of millimeter to centimeter-sized aggregates in the solar nebula (Weidenschilling and Cuzzi, 1993; Weidenschilling, 1997). The results will provide insight into current aggregation theories, as well as increase our knowledge on the initial conditions and clumping properties leading to the creation of planetary systems.

On ESA's 45$^{\mathrm{th}}$ Parabolic Flight Campaign we investigated the collision behavior of RBD dust aggregates (Blum and Schräpler, 2004; Blum et al., 2006) at room temperature corresponding to a distance of 1 AU (the distance of Earth's orbit to the sun) from the protostar (Wood, 2000). In two more Parabolic Flight Campaigns, scheduled for November 2007, we will continue our experiments to probe collisions and impacts of similar dust aggregates at low temperatures of $140-250$ K ($2-5$ AU) and we will perform collisions using icy samples at cryogenic temperatures (≤ 140 K), similar to those in the outer protoplanetary nebula ($5-30$ AU).

4 Experiment Setup

To investigate the collisions of millimeter-sized dust aggregates and icy bodies under conditions comparable to the early solar nebula an experimental setup was designed to allow a large number of collisions at temperatures of $80-300$ K. Therefore, a sample storage for 180 projectiles was fit onto a thermal reservoir (Sect. 4.1) which keeps the desired temperatures for the duration of the experiment (see the CAD drawing in Fig. 1). To prevent the fragile dust aggregates from being damaged by acceleration of more than $10\,g_0$ (where $g_0 = 9.81\,\mathrm{m\,s^{-2}}$, Earth's gravitational acceleration) a smooth particle acceleration (Sect. 4.2) mechanism was developed. To probe collisions of different sized bodies, a target frame – simulating a larger aggregate – is installed in the center of the collision volume (Sect. 4.3). The collision events are recorded by a high-speed, high-resolution digital recording system (Sect. 4.4) attached to the vacuum chamber's top flange. The vacuum chamber (housing the collision volume and the sample repository) and all diagnostic hardware are installed into two custom-made aluminum racks to comply with the safety requirements for parabolic flights.

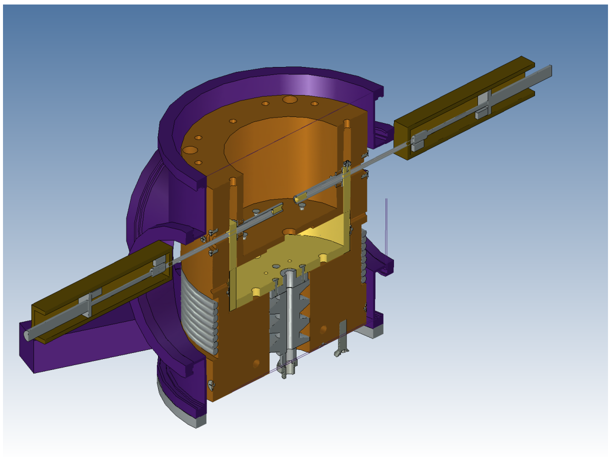

Figure 1: Cross-section of the experiment chamber. At left and right, two hydraulic actuators are attached. In the center, the shielded sample repository is fit onto the thermal reservoir.

4.1 Thermal Reservoir and Particle Storage

To keep the experiment at the desired low and cryogenic temperatures for the duration of one parabolic flight a thermal reservoir is mandatory, since no liquid Nitrogen (N_2) is allowed aboard the Zero-G aircraft. Therefore, the experiment is equipped with a massive, 50 kg copper block which is fit into a cylindrical vacuum chamber of 290 mm $\times$ 250 mm. The thermal reservoir is cooled by liquid N_2 spiraling through a copper tube wound around the copper block and attached to a liquid N_2 feedthrough at the bottom flange of the vacuum chamber. Cooled down to cryogenic temperatures the warm-up rate of the system is $\lesssim 5\,\mathrm{K}$ per hour. To avoid heat transfer by thermal conductivity of the residual air inside the vacuum chamber a dry, oil-free membrane pump and a turbo molecular pump (TMP) are operated in series to keep the pressure at $p \leq 10^{-3}\,\mathrm{mbar}$.

If access to the interior vacuum chamber is required, the thermal reservoir and the attached collision volume can be heated up to ambient temperature using 34 meters of heat rope with a maximum power of 840 W which is wound around the copper block.

On top of the thermal reservoir one of two cylindrical sample repositories (Fig. 2) – made from copper or aluminum, respectively – is attached to a brass-made quintuple thread which is fit to a bore in the center of the copper block, thereby establishing good thermal contact to the reservoir.

The sample carrier offers space for storing 180 projectile aggregates which can be placed inside a double-helix of 90 holes each. Thus, 90 collisions of pairs of aggregates or 180 impacts of aggregates with a larger target can be performed by manually rotating the cylindrical storage. In order to prevent the projectiles from falling out of the storage compartments, and for shielding the aggregates from radiative warming, a copper-made lid covers the sample repository.

4.2 Particle Acceleration Mechanism

To study collisions in the velocity range $0.1\,\mathrm{m\,s^{-1}} \lesssim v_c \lesssim 0.5\,\mathrm{m\,s^{-1}}$, which is of astrophysical relevance (Weidenschilling and Cuzzi, 1993; Weidenschilling, 1997), the aggregates are accelerated by a set of synchronized, hydraulic pistons. The hydraulic actuators are driven by an electrical DC motor at constant acceleration level which ensures that the projectiles do not experience accelerations exceeding $10\,g_0$. The two hydraulic pistons are mounted opposite each other at the outside of the vacuum chamber, and are guided to the sample repository passing through a mechanical feedthrough, followed by a guiding PTFE* piece, until they pick up the projectiles. To prevent the aggregates from falling off the conical stainless steel rods they are accelerated through guiding tubes of 80 mm length until the pistons reach their outmost position, where switches are activated to abruptly stop and rapidly retract them.

4.3 Removable Collision Target

In addition to particle-particle collisions, a target screen (Fig. 3), in which micron-sized dust grains can be packed to simulate the surfaces of larger protoplanetary bodies, is used to probe

*Polytetrafluoroethylene

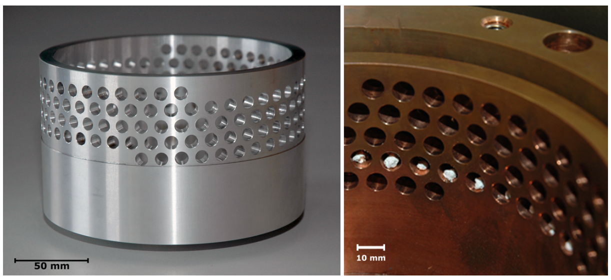

Figure 2: The cylindrical sample reservoir offers storage capacity for 180 individual millimeter-sized projectiles. On the left, the aluminum-made sample repository and to the right, the partly filled individual compartments of the copper reservoir.

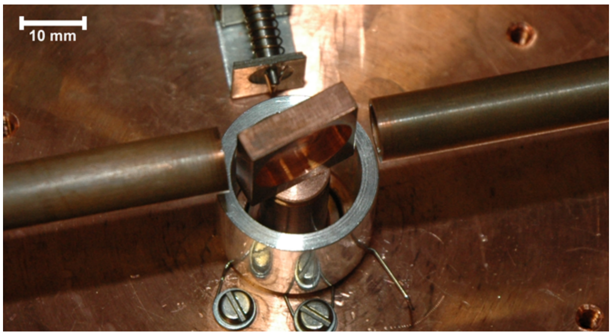

Figure 3: Pivot-mounted target frame in the collision volume (center). To the left and right of the target two cylinders are visible, within which the projectiles are accelerated from their storage compartments. In the center top of the image the target-release-mechanism can be seen, where the target can be lowered out of the collision volume during flight to allow for aggregate-aggregate collisions.

collisions of small particles with larger ones.

A mould of 17 mm diameter and 2 mm depth is machined in either side of a copper frame, and installed between the two guiding tubes at the center of the collision volume and there attached to the sample repository. To vary the impact angle, the target screen rotates by eight degrees per collision (separation between neighboring storage compartments). Thus, almost arbitrary impact angles in the range $0° - 75°$ (limited by the edges of the target frame blocking the exits of the guiding tubes) can be achieved. Additionally, a solenoid release mechanism offers the opportunity to drop the target to a fixed position at the bottom of the collision volume and thus, allows us to switch to particle-particle collisions.

4.4 Imaging and Data Acquisition

Recording of image sequences of the collisions is done by a high-speed, high-resolution CMOS** camera and a high-performance recorder computer. The camera was operated at a continuous accumulation of 107 fps of 8 bit grayscale images of 1280×1024 px. Thus, the field-of-view covers a plane of $24 \times 20\,\mathrm{mm}^2$ at a focal depth of ~ 5 mm. The recording system is capable of writing images at a maximum data rate of $133\,\mathrm{MByte\,s^{-1}}$ to its 4 hard disks (totalling 260 GByte), corresponding to a maximum recording time of 33 minutes.

To capture the collisions the camera is mounted to a viewport at the vacuum chamber's top flange. The collision volume is illuminated by two synchronized stroboscopic (Xenon) flash lamps which are also synchronized with the camera's image acquisition at 107 Hz.

Complementary **Metal **O**xide **S**emiconductor

5 Microgravity Experiments

During ESA's 45$^{\mathrm{th}}$ Parabolic Flight Campaign collision experiments were carried out at ambient temperatures (~ 300 K) and a pressure of $2.8 \cdot 10^{-1}$ mbar. Projectiles were prepared from 2.5 cm RBD dust aggregates built from monodisperse 1.5 μm-sized SiO_2 grains. The $2 - 5$ mm dust aggregates were cut from the larger 'dust cakes' using a razor blade. Recent x-ray tomography measurements showed that at the cutting edges of the dust aggregates a slight compaction from $\phi = 0.15$ to $\phi \approx 0.17$ can be observed.

These projectiles were used to perform $3 - 4$ collisions per parabola. Thus, images sequences of 76 impacts of dust aggregates against a compact dust target of $\phi = 0.24$ could be recorded (see Fig. 4 for an example). It was observed that in $\sim 90\%$ of the impacts the projectiles bounced off the target, whereas $\sim 10\%$ of the collisions resulted in sticking of – only very small – projectiles. Fragmentation was negligible for this type of experiment.

In addition to the particle-target collisions, 39 encounters of pairs of fluffy dust aggregates were captured (see Fig. 5 for an example). Analysis of the image sequences showed that again $\sim 90\%$ of the collisions were dominated by rebounding behavior. For this type of experiment fragmentation was observed in $\sim 10\%$ of the collision events, whereas in this case sticking was unimportant.

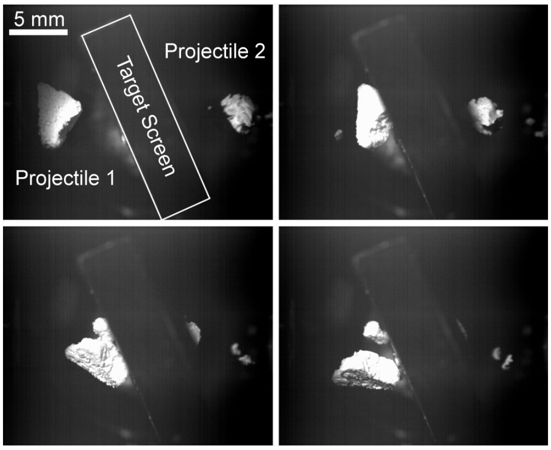

Figure 4: Example of a collision of a high-porosity dust aggregate with a compact dust target. The collision velocity is $\sim 0.2\,\mathrm{m\,s^{-1}}$. The time between subsequent images is 19 ms.

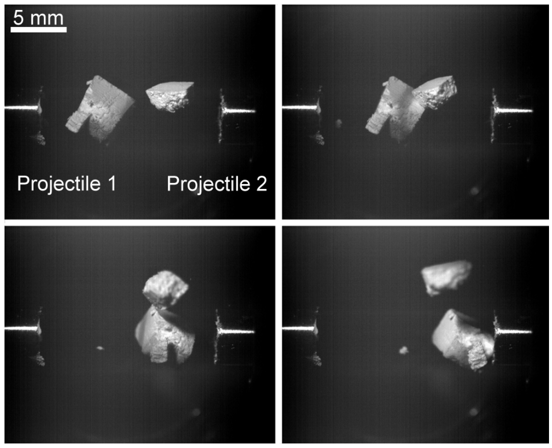

Figure 5: Example of a collision between two high-porosity dust aggregates. The collision velocity is $\sim 0.4\,\mathrm{m\,s^{-1}}$. The time between subsequent images is 19 ms.

Analysis of the relative velocities of the colliding bodies before and after the impact, calculation of the coefficient of restitution and determination of the normalized impact parameter (for aggregate-aggregate collisions) and impact angle (for aggregate-target collisions), respectively, show that for a central collision only $\sim 5\%$ of the translational energy is conserved. This value increases with increasing normalized impact parameter. Additionally, from the image sequences it becomes clear that a significant amount of energy is transformed into rotational motion of the aggregates after the encounter. A quantitative analysis could not be performed, because the narrow depth of field, and thus, blurring effects ruled out the determination of the rotational velocity and the irregular shape of the aggregates made a determination of the moment of inertia impossible.

6 Experiment Improvements for Future Campaigns

To improve the experimental setup and to increase the quality of the obtained data for future Parabolic Flight Campaigns a number of changes will be or were already made. During ESA's 45$^{\text{th}}$ PFC only the copper-made sample repository was used. In order to save valuable time during preparation of the parabolic flights a second, aluminum-made sample reservoir was machined. This can be prepared for the upcoming flight by the ground crew, while the flight crew uses the other one to perform microgravity experiments. Thus, the optimized procedures are expected to save 2.5 hours of preparation time between subsequent flights.

Additionally, to increase the quality of the recorded image sequences and remove any shadowing effects the stroboscopic illumination will be modified by mounting two synchronized flash lamps at an angle of $\alpha = 45°$ to the pistons' axis and at an angle of $\beta = 56°$ to the camera axis. The high-speed camera will be extended by a beam splitter optics which allows to record image sequences with an angular separation of $\psi = 60°$. Thereby, three-dimensional collision information – allowing the exact determination of the impact parameter – can be obtained.

To optimize the separating of the projectile from the pistons' conical heads the hydraulic acceleration mechanism will be replaced by a synchronized master-and-slave system of electric DC motors. In contrast to the previously used hydraulic ones, these motors with their attached leadscrews will be equipped with a hard, mechanical stop confirming the instantaneous deceleration of the pistons' rods allowing a more accurate separation of the aggregates.

Acknowledgments

We thank J. Barrie (University of Strathclyde), G. Borst (Dutch Space), M. Costes (University of Bordeaux I), R. W. Dawson (University of Strathclyde), G. Drinkwater (University of Strathclyde), F. Gai (Novespace), K. Gebauer (Technical University at Braunschweig), J. Gillan (University of Strathclyde), M. Hutcheon (University of Strathclyde), E. Jelting (Technical University at Braunschweig), L. Juurlink (Leiden University), M. Krause (Technical University at Braunschweig), E. de Kuyper (Leiden University), H. Linnartz (Leiden University), J. Lub (Leiden University), F. Molster (NOVA), A. Orr (ESA), D. Salter (Leiden University), B. Stoll (Technical University at Braunschweig), P. Tuijn (Leiden University), G. van der Wolk (University of Groningen) and the members of the ESA Topical Team: Physico-Chemistry of Ices in Space, ESTEC Contract No: 15266/01/NL/JS.

The project was generously supported by Air Liquide, Kayser-Threde GmbH, Pfeiffer Vacuum, the Radboud University Nijmegen and VTS Ltd.

The ICES experiment was co-funded by the German Space Agency (DLR) under grant No. 50 WM 0636, the European Space Agency (ESA), the Leids Kerkhoven-Bosscha Fonds (LKBF), the Netherlands Research School for Astronomy (NOVA), the Netherlands Institute for Space Research (SRON) under grant No. PB-06/053 and the Scottish Universities Physics Alliance (SUPA) Astrobiology Equipment Fund.

We are indebted to the late Ron Huijser for many stimulating discussions.

References

Blum, J.: 2004, Grain Growth and Coagulation, *in* A. N. Witt, G. C. Clayton and B. T. Draine (eds), *Astrophysics of Dust*, Vol. 309 of *Astronomical Society of the Pacific Conference Series*, p. 369.

Blum, J. and Münch, M.: 1993, Experimental investigations on aggregate-aggregate collisions in the early solar nebula, *Icarus* **106**, 151.

Blum, J. and Schräpler, R.: 2004, Structure and Mechanical Properties of High-Porosity Macroscopic Agglomerates Formed by Random Ballistic Deposition, *Physical Review Letters* **93**(11), 115503.

Blum, J., Schräpler, R., Davidsson, B. J. R. and Trigo-Rodríguez, J. M.: 2006, The Physics of Protoplanetesimal Dust Agglomerates. I. Mechanical Properties and Relations of Primitive Bodies in the Solar System, *The Astrophysical Journal* **652**, 1768.

Blum, J. and Wurm, G.: 2000, Experiments on Sticking, Restructuring, and Fragmentation of Preplanetary Dust Aggregates, *Icarus* **143**, 138–146.

Bridges, F. G., Hatzes, A. P. and Lin, D. N. C.: 1984, Structure, stability and evolution of Saturn's rings, *Nature* **309**, 333–335.

Brown, R.: 1828, A Brief Account of Microscopical Observations Made in the Months of June, July, and August, 1827, on the Particles Contained in the Pollen of Plants; and on the General Existence of Active Molecules in Organic and Inorganic Bodies, *Edinburgh New Philosophical Journal* pp. 358–371.

Dominik, C. and Tielens, A. G. G. M.: 1997, The Physics of Dust Coagulation and the Structure of Dust Aggregates in Space, *The Astrophysical Journal* **480**, 647.

Ehrenfreund, P., Fraser, H. J., Blum, J., Cartwright, J. H. E., García-Ruiz, J. M., Hadamcik, E., Levasseur-Regourd, A. C., Price, S., Prodi, F. and Sarkissian, A.: 2003, Physics and chemistry of icy particles in the universe: answers from microgravity, *Planetary and Space Science* **51**, 473.

Einstein, A.: 1905, Über die von der molekularkinetischen Theorie der Wärme geforderte Bewegung von in ruhenden Flüssigkeiten suspendierten Teilchen, *Annalen der Physik* **322**, 549–560.

Fraser, H. J., Ehrenfreund, P., Blum, J., Cartwright, J. H. E., Hadamcik, E., Levasseur-Regourd, A. C., Price, S., Prodi, F., Sarkissian, A. and Seurig, R.: 2005, Ices in the Universe: Answers from Microgravity, *ESA Special Publication* **1281**, 52–76.

Hatzes, A. P., Bridges, F. G. and Lin, D. N. C.: 1988, Collisional properties of ices spheres at low impact velocities, *Monthly Notices of the Royal Astronomical Society* **231**, 1091–1115.

Krause, M. and Blum, J.: 2004, Growth and Form of Planetary Seedlings: Results from a Sounding Rocket Microgravity Aggregation Experiment, *Physical Review Letters* **93**(2), 021103.

Langkowski, D., Teiser, J. and Blum, J.: 2007, The Physics of Protoplanetesimal Dust Agglomerates: II. Low Velocity Collision Properties. Submitted to *The Astrophysical Journal*.

Meakin, P. and Donn, B.: 1988, Aerodynamic properties of fractal grains - Implications for the primordial solar nebula, *The Astrophysical Journal* **329**, L39–L41.

Weidenschilling, S. J.: 1997, The Origin of Comets in the Solar Nebula: A Unified Model, *Icarus* **127**, 290.

Weidenschilling, S. J. and Cuzzi, J. N.: 1993, Formation of planetesimals in the solar nebula, *in* E. H. Levy and J. I. Lunine (eds), *Protostars and Planets III*, p. 1031.

Wetherill, G. W. and Stewart, G. R.: 1989, Accumulation of a swarm of small planetesimals, *Icarus* **77**, 330–357.

Wetherill, G. W. and Stewart, G. R.: 1993, Formation of planetary embryos - Effects of fragmentation, low relative velocity, and independent variation of eccentricity and inclination, *Icarus* **106**, 190.

Wood, J. A.: 2000, Pressure and Temperature Profiles in the Solar Nebula, *Space Science Reviews* **92**, 87–93.

Wurm, G. and Blum, J.: 1998, Experiments on Preplanetary Dust Aggregation, *Icarus* **132**, 125.